Article

Removal of methyl orange dye pollutant from aqueous solution by ghraphene oxide/ sodium algirate nono composite

Liqaa Ismael Ali and Dhia H. Hussain

Department of chemistry /College of Sciences /Mustansiriyah University.

Abstract

In order to provide inexpensive and efficient technique for wastewater treatment, the present research, aimed to prepare nano composites out of graphene oxide, namely GO/SA aerogels and focused on its application to remove methyl orange dye from industrial wastewater. Energy dispersive X-ray analysis (EDX), field-emission scanning electron microscopy (FE-SEM), and X-ray diffraction (XRD) were employed to identify the compound of GO/SA composite aerogel. High porosity was shown in nanomaterials, sample purity was demonstrated by EDX analysis, and the impact of temperature on dye absorption was investigated. In other words, the process is endothermic, as the data revealed that raising the temperature improved absorption efficiency. The results conclude that the GO/SA composite aerogel can be an effective adsorbent for eliminating the pollutants such as dyes from an aqueous environment.

Keywords: Graphene oxide; aerogel; Nano-material; Polymer; Dye removal

Introduction

Nowadays, water pollution is a major environmental problem that negatively affects the aquatic species and biological community. The environmental pollution problems emerge as a side effect of the industrial activities' growth [1]. The main classes of water pollutants are organic contamination such as hazardous dyes coming from industrial wastewater [2]. Among these dyes, Methyl orange is a very common water-soluble dye that is vastly used in various industries such as textile industry [3]. Methyl orange dye has carcinogenic and toxic effects on human and aquatic environment

[4,5]. Therefore, it is essential to remove this dye from industrial wastewater before discharging it into aqueous environment. So far adsorption is a rabid, low cost and high effective method used for treating and eliminating the organic dyes from industrial wastewater which has drawn a great attention of scientists [6-8]. Through this technique, dye molecules adhere to the surface of adsorbent (solid material) by physical or chemical interactions [9]. There are various factors that affect the procedure of wastewater treatment by adsorption including pH solution, temperature, and adsorbent concentration [10,11]. Graphene oxide (GO) is the most attracted dye adsorbents in wastewater treatment due to its unique conjugated formation which provides higher capacity of adsorption for different dye particles by π-π interactions and their key features including large surface area and several oxygen-based functional groups (i.e., carboxy, carbonyl, hydroxyl groups) [12-15]. Hummer's method is the most common method used to synthesize GO from graphite [16]. However, GO particles exhibit a high tendency to agglomerate and they are difficult to disperse in water as it decreases the adsorption technique efficiency [17-19]. It has been reported that GO can be a great constituent for efficient nano-composites in treatment of pollutants [20,21]. To achieve enhanced adsorption performance by facilitating the separation of dyes adsorbed-GO from water, porous graphene oxide aerogel (GO/SA) was introduced in this study in a composited form. The nano-composites were obtained using the process of freeze-drying. Freeze-drying is a common technique for obtaining GO/SA with a unique look, similar to molds [22].

Currently, aerogel has become very vital in terms of removing different types of pollutants for example heavy metals, radioactive elements and dyes [23-26]. Aerogels are a specific class of 3D substance with high porosity, a high specific surface area, as well as low density and thermal conductivity [27]. Thus, aerogels are considered superior adsorbents due to their particular properties and their highest adsorption capacity [28]. There is a wide range of chemical substances that may be used to create aerogels [29]. They are made by supercritical drying or freeze-drying gel to remove the liquid component. Because of this, the liquid may be evaporate slowly without causing the solid matrix in the gel to collapse as a result to capillary action. Up to date, there are different types of aerogel molecules that have been suggested to treat wastewater. This study focuses on graphene oxide based aerogel that is the most commonly used. GO/SA composite aerogel was prepared and the prepared nano-composite structure was identified by X-Ray diffraction, field-emission scanning electron microscopes (FE-SEM) and energy dispersive X-Ray analysis (EDX). Methyl orange dye adsorption with this synthesized nano-composite was studied in a package of experiment. The impact of experimental parameters including Methyl orange dye concentration in solution, pH, and temperature was evaluated

Methodology

Preparation of adsorbate

Methyl orange dye (Sodium4- {[4 (diethylamino) phenyl] diazenyl} benzene-1-sulfonate) with molecular weight of 327.34 gm/mol, was used as adsorbate. The stock solutions of Methyl orange were prepared through dissolving 0.02 gm of dyes in 1000 ml distilled water. After that, a series of solutions with desired concentration was prepared by sequential dilution of methyl orange stock with deionized water at suitable volume. UV-visible spectrophotometer was used to analyzed the aqueous solution of methyl orange. The wavelength corresponding to maximum absorbance was at 464 nm.

Preparation of GO/SA composite aerogel

Graphene oxide was prepared using Hummer's method [16,30]. Preparation of GO/SA composite aerogel was achieved by using an ultrasonic bath. For 1 hour, 0.32 gm of dried GO (8 mg/ ml) [35] was equally disseminated in 40 ml of deionized water. This was followed by the addition of 0.32 gm, 0.96 gm, and 1.6 gm of SA. After 30 minutes of cross-linking with Ca^{+2}, hydrogel beads were made by injecting the homogeneous solution drop by drop into the $CaCl_2$ (2 wt.%) solution [31]. To make GO/SA aerogel, the hydrogel beads were first washed five times in deionized water. Then, they were vacuum freeze-dried for 72 hours.

Use of GO/SA aerogel as adsorbents

To choose the most suitable model for adsorption, A 0.01 gm of each the three prepared GO/SA aerogel samples were added to 10 ml of the standard solution of methyl orange dye (20ppm). The solutions were filtered and the absorbance of the filtered solution was then measured by UV-Vis at 464 nm.

Time required for equilibrium

Equilibrium time was determined by preparing 6 solutions (20 ppm) of methyl orange dye, (0.01 g) of GO/SA aerogel was added to each dye (20 ppm) solution. Samples were taken (with filtering) to measure the change in concentration every 15 minutes for up to 90 minutes (15, 30, 45, 60, 75, 90 minutes). They were stirred continuously during this process at 185 rpm at a temperature of 25°C, the absorbance was measured after adsorption using a UV-Vis spectrometer at a wavelength of 464 nm. Experiments showed that the equilibrium time was (75 minutes) for the GO/SA aerogel. [31].

Effect of pH

This parameter was established by adding 0.01 gm of GO/SA aerogel, to 3 flasks containing a certain concentration of methyl orange dye (20 ppm), to prepare 3 solutions with the same concentration but different in acidity functions (4, 7, 9 pH). GO/SA aerogel samples were kept on a magnetic stirrer for 75 minutes at 25°C and 185 rpm. The solutions were then filtered and the absorbance was then measured after adsorption using a UV-Vis spectrometer at 464 nm [32].

Effect of adsorbate concentration

Various concentrations of methyl orange dye (2, 4, 8, 12, 16 ppm) were used to examine the impact of varying adsorbate concentration on the adsorption process. A 0.01g of adsorbent (GO/SA aerogel severally) was added to each of the above concentrations. Continuous stirring at speed of 185rpm and temperature of 25°C for 75 minutes was done for GO/SA aerogel. Finally, the mixing solutions were filtered and their absorbance was measured at 464 nm [33]. The dye removal rate and the amount of adsorbate were calculated according to the following equations (1-2), (2-2).

$R\% = 100[Ci - (Ce/Ci)]$ …………………………………… (2-1)
$Qe = [Ci - Ce]\, V/m$ ………………………………………… (2-2)

Where the R is a removal rate, C_e is the residual concentration of the dye in ppm (mg/l), C_i is the initial concentration of the dye in ppm (mg/l), Qe is amount of adsorption in (mg/g), V is the volume of the dye solution in (L) and m is the weight of the nanomaterial.

Temperature effect

This parameter was investigated using 0.01gm of the adsorbent (GO/SA aerogel severally), which was added to 5 solutions of methyl orange dye at same concentration but different temperatures (15, 25, 35, 45 and 55). Continuous stirring at a speed of (185 rpm) and temperature of 25°C for 75 minutes in case of GO/SA aerogel. Finally, the sample solutions were filtered and their absorbance was measured at 464 nm.

Effect of adsorbent weight on adsorption

Five dye solution samples at a concentration of 20ppm were prepared in 100 ml volumetric flasks. Nanomaterials with different weights in grams (0.01, 0.02, 0.03, 0.04, 0.05) were added materials to each solution. The five flasks were placed in a water bath with continuous stirring at a speed of 185rpm and temperature of 25°C for 75 minutes in case of GO/SA aerogel. The nanoparticles were filtered and the absorbance was measured using a UV-Vis spectrometer at 464 nm.

Result and discussion

Characterization of GO/SA aerogel

X-ray Diffraction Analysis (XDR)

The structural information of prepared nanocomposites was verified using the powder X-ray diffraction technique. All the scans have been recorded by SHIMADZU XRD-6000. The XRD uses a monochromatic Cu Kα radiation line of wavelength (λ =1.54 ˚A) in 2θ range from 10◦ to 80◦, at 25 °C. The CuKα radiation source was set at 40 kV voltage and 30 mA current and the scanning speed of 10°/min. The X-ray diffraction patterns shown in Figure 1 the diffraction peaks appeared at 12.22°, which were corresponding to the characteristic peak of GO. The peak at 2θ = 12.22° of GO corresponded to the (001) crystal plane reflection of GO. Another peak was observed at the 2θ = 42.49°, belongs to the crystal plane (100) [34]. Figure 2 displays the XRD patterns of GO/SA aerogel. GO has a diffraction peak at 2θ = 11.0°. The broad peak of SA at 2θ =13.6° demonstrates the amorphous nature of SA in general [35, 36]. XRD pattern displays tetragonal shape of GO nanoparticles and the bandwidth refers to the small size of the crystal. [37].

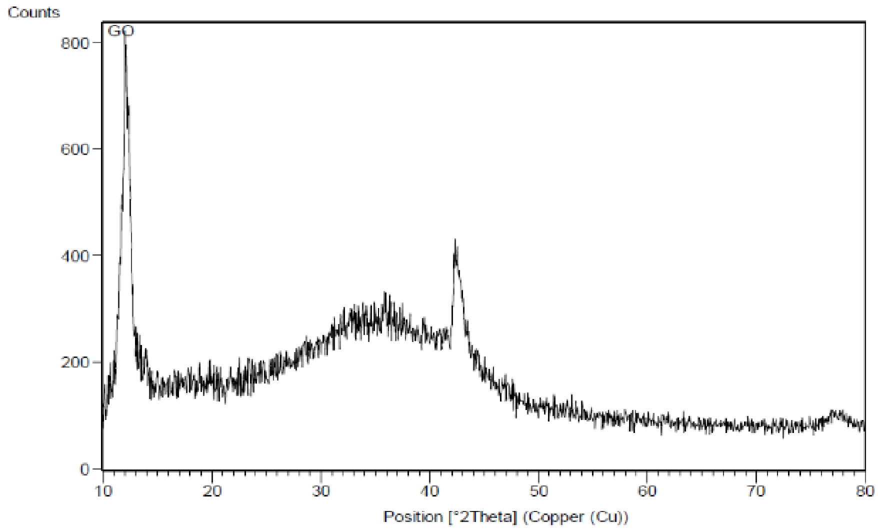

Figure 1: X-ray diffraction pattern of Graphen Oxide (GO)

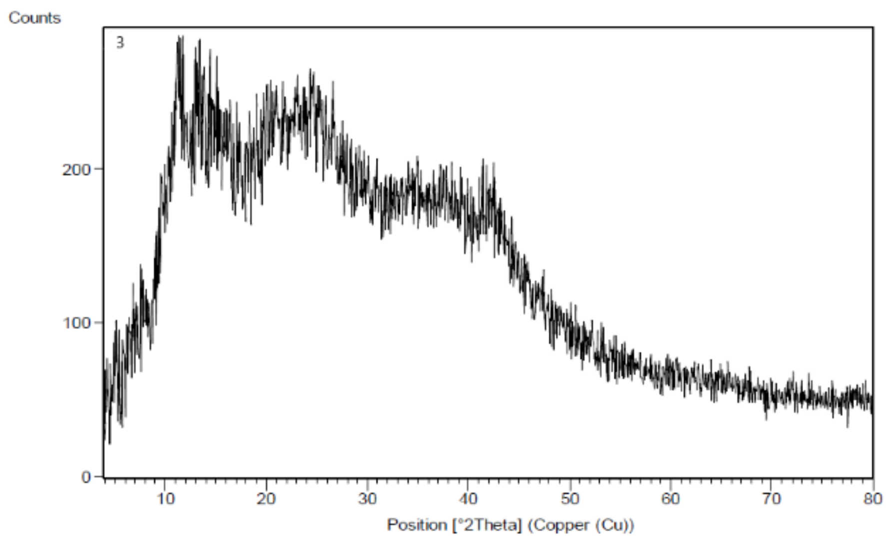

Figure 2: X-ray diffraction pattern GO/SA aerogel.

Field Emission Scanning Electron Microscopy (FE-SEM)

The morphological features and the shape of synthesized nanomaterials as examine by FE-SEM analysis. Figures 3 (A&B) and 4(A&B) represents the FE-SEM analysis at different magnifications for synthesized nanomaterials GO and GO/SA aerogel nanosheet respectively [38]. The two-dimensional structure of the GO nanosheet, and GO/SA aerogel is clearly appeared; it shows the surface of GO nano-sheets with a layer of wrinkles forming one on top of another, and the GO/SA NPs with different sizes depend on the surface of graphene oxide

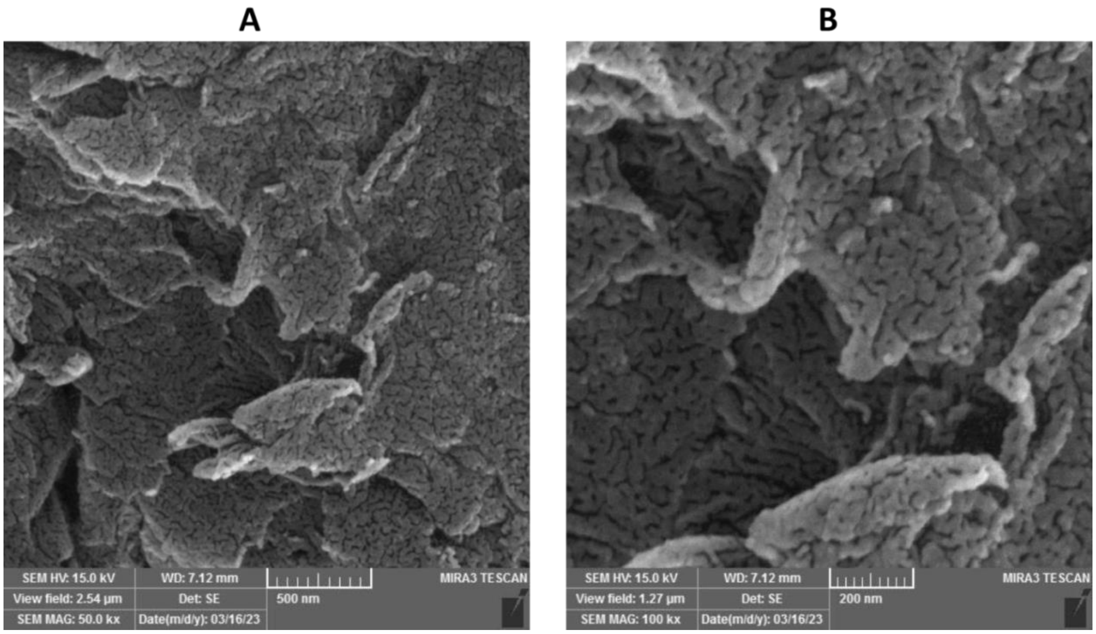

Figure 3: FE-SEM images of GO (Nanosheet) at different magnification (A and B).

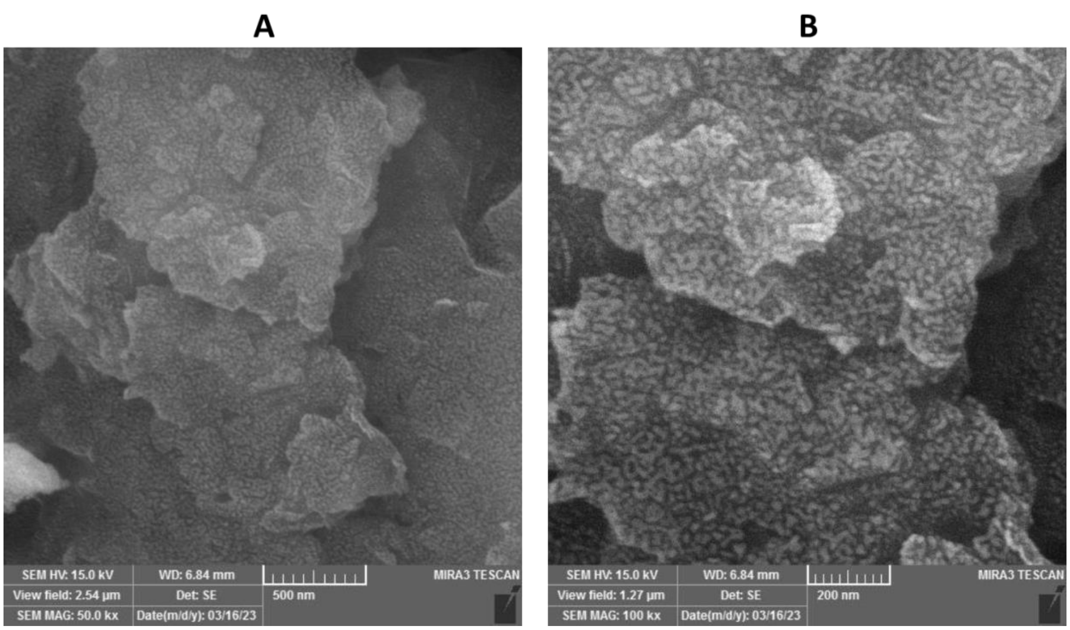

Figure 4: FE-SEM images of GO/SA aerogel (NPs) at different magnification (A and B).

Energy Dispersive X-Ray Analysis (EDX)

The EDX technique was used to determine the chemical composition of the prepared nanomaterials GO, and GO/SA composite aerogel. A sample of graphene oxide nanoparticles contains carbon, oxygen, sulfur and a sample of graphene oxide aerogel nanoparticles contains elements oxygen, carbon and sulfur. The presence of the sulfur element in the spectrum was due to the fact that the graphene oxide had not been washed well during its preparation process, and residues of sulfuric acid remained in the powder [39]. The proportions (percentage) of the elements in the samples were obtained, in agreement with what was calculated theoretically for each element in the studied samples as shown in Table (1&2). Figures 5 and 6 show the EDX map images of nano-composite GO and GO/SA aerogel that display a map of the distribution of atoms for each element in two samples. This study has found that the atoms are distributed homogeneously in the map of each sample and that atoms are uniformly scattered on the surface sample, which indicates that the atoms take multiple places in the sample, giving wide space for diffusion. This is one of the properties of nanomaterials, as they have smaller sizes and a wide surface area.

Table 1: Quantitative results of EDX image of GO(Nanosheet)

Elt	Line	Int	Error	K	Kr	W%	A%	ZAF	Ox%	Pk/Bg	Class	LConf	HConf	Cat#
C	Ka	607.4	3.4353	0.6509	0.2633	53.12	61.06	0.4957	0.00	268.29	A	51.60	54.63	0.00
O	Ka	447.1	3.4353	0.2752	0.1113	43.38	37.44	0.2566	0.00	116.40	A	41.94	44.82	0.00
S	Ka	195.2	13.3160	0.0739	0.0299	3.50	1.51	0.8549	0.00	11.47	A	3.32	3.67	0.00
				1.0000	0.4046	100.00	100.00		0.00					0.00

Table2: Quantitative results of EDX image for GO/SA aerogel (NPs).

Elt	Line	Int	Error	K	Kr	W%	A%	ZAF	Ox%	Pk/Bg	Class	LConf	HConf	Cat #
C	Ka	233.7	2.9171	0.3621	0.1393	40.29	51.69	0.3457	0.00	84.93	A	38.44	42.14	0.00
O	Ka	295.2	2.9171	0.2627	0.1011	42.94	41.36	0.2354	0.00	61.33	A	41.19	44.69	0.00
S	Ka	100.8	3.5101	0.0552	0.0212	2.41	1.16	0.8809	0.00	4.53	A	2.24	2.58	0.00
Cl	Ka	195.4	3.5101	0.1188	0.0457	5.42	2.35	0.8439	0.00	12.61	A	5.15	5.69	0.00
Ca	Ka	239.5	0.9990	0.2011	0.0774	8.94	3.44	0.8648	0.00	17.01	A	8.54	9.35	0.00
				1.0000	0.3847	100.00	100.00		0.00					0.00

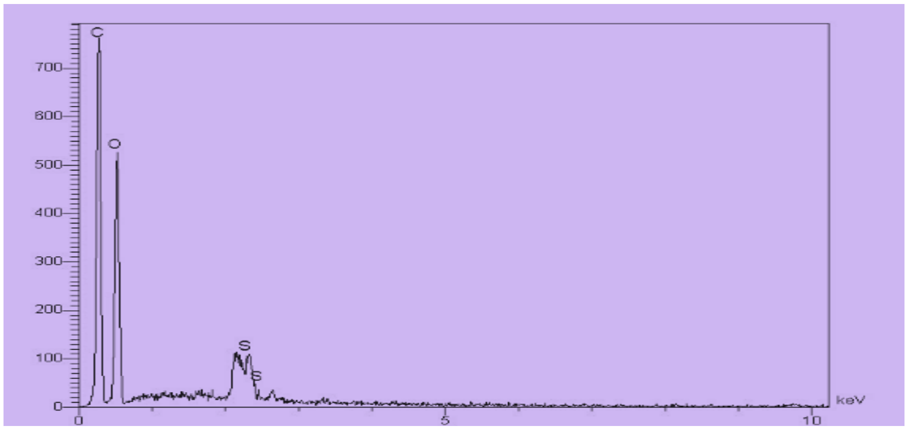

Figure 5: EDX spectra of GO (Nanosheet).

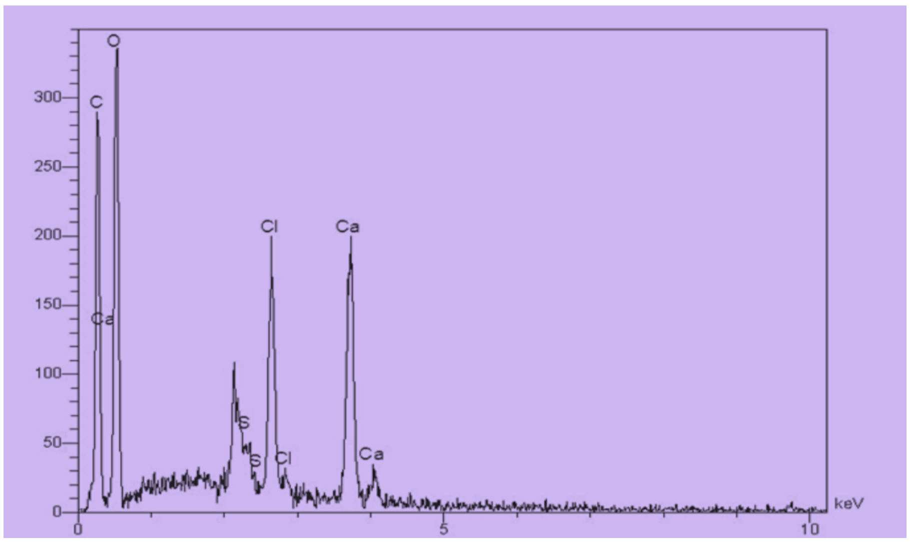

Figure 6: EDX spectra GO/SA aerogel (NPs).

Batch adsorption results

In order to achieve the adsorption efficiently, different experimental parameters were investigated including pH solution, contact time, and adsorbent mass (weight), Dye concentration and temperature.

Effect of contact time

The important parameter that influences the adsorption of methyl orange on the GO/SA aerogel nano-composite is reaction time which was studied at 25 °C. Figure 7 displays the impact of the contact time on the removal percentage and adsorption efficiency of the composite at time intervals (15–120 min). The methyl orange dye concentration was (2–20 ppm) in a volume of 10 ml and the amount of nanomaterials added (0.01 gm). From (185 revolutions per minute), it was observed that the methyl orange removal percentage increased with increasing contact time until it reaches a steady state at 75 min in which all sites on the surface of adsorbent nanoparticles are steadily occupied and the adsorption process slows down to eventually levels off [40]. This is corresponded to complete removal percentage of 46.79% at the time of the equilibrium for GO/SA aerogel nanocomposites.

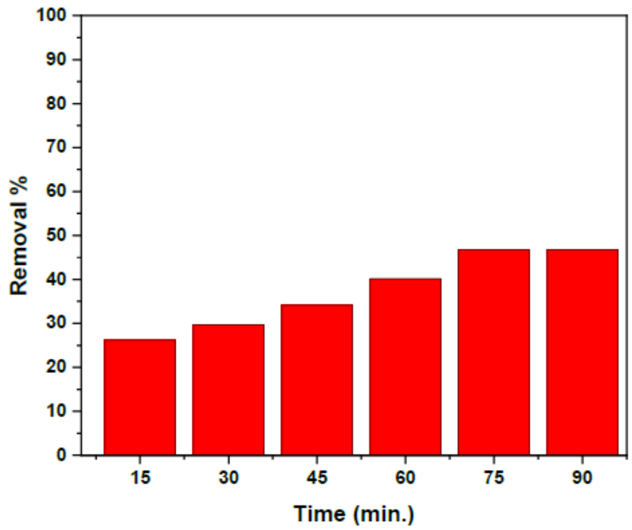

Figure 7: The effect of contact time on the adsorption of methyl orange on GO/SA aerogel. nano composite

Effect of adsorbent mass

The effect of adsorbent weight on the adsorption of methyl orange dye was studied using GO/SA composite aerogel mass rang (0.01-0.1) gm at a temperature of 25 °C with constant stirring in a water bath (185rpm). Figure 8 shows the removal rate of methyl orange dye adsorbed with different amounts of GO/SA composite aerogel. The results showed that while increasing the weight of the adsorbent material the adsorption increases. This is due to the increased availability of adsorbent surface area and active sites offered at greater mass. The excessive active sites formation on the GO/SA aerogel nanocomposite at higher weight of adsorbent leads to an increase in the removal percentage of the dye. The highest removal percentage at the weight of (0.1 gm) for the GO/SA aerogel nanoparticles is 92%, and this is a normal behavior for nanomaterials. In terms of the economic point of view and the performance of adsorption, 0.1 gm/L of adsorbent would be useful as the ideal dosage for application.

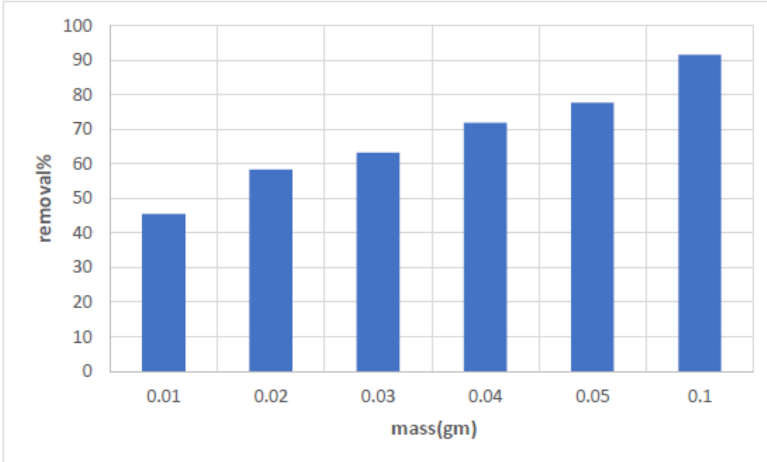

Figure 8: Effect of GO/SA aerogel nanocomposite mass on dye adsorption.

Effect of initial dye concentration

The effect of the initial concentration of the prepared dye on the adsorption process was studied by combining 0.01 g of GO/SA aerogel nanocomposites with different dye concentrations ranging 2-20 ppm for methyl orange at a temperature of 25 °C and with contact time of 75 minutes. The results reveal that by increasing the dye concentration from 2 to 20 ppm, the removal efficiency percentage of prepared GO/SA aerogel nanocomposites began to decrease from 88% -25%. The reduction in removal efficiency is attributed to higher concentrations of methyl orange, since the adsorbate occupies all the multilayers of the adsorbent surface, resulting in lower adsorption efficiency. Figure 9 shows the removal rate of different dye concentrations on the prepared GO aerogel nano surfaces.

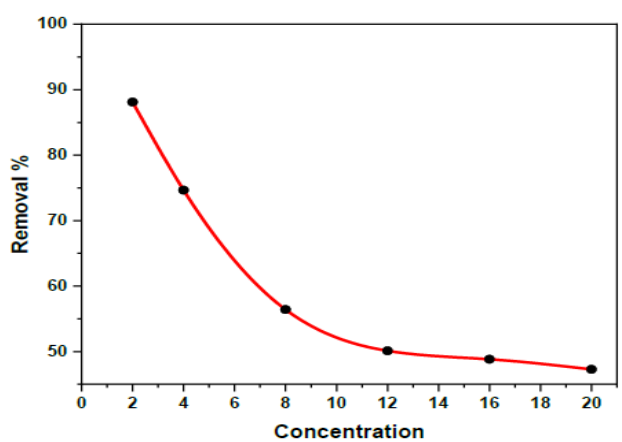

Figure 9: Effect of dye concentration on adsorption on the surface of GO/SA aerogel.

Effect of Temperature

Temperature is significant parameter to recognize the nature of the adsorption system. The effect of temperature on the adsorption of methyl orange dye on surface of GO/SA composite aerogel nanomaterials was investigated at the temperature ranging 15-55 °C with (it suppose initial conc) dye concentration (2-20 ppm) onto 0.01 gram of the prepared GO/SA aerogel nanomaterials, in 10 ml volume at contact time 75 min and shaking speed 185rpm. The effect of temperature on adsorption efficiency of GO/SA aerogel nanocomposites for methyl orange dye is displayed in Figure 10. According to the observed data, the removal rate increased from 33% to 47.28% with increasing temperature from 290 t0 300k. Achieving a high removal efficiency is due to an increase in both the surface energy and molecular diffusion of the dye on the surface of adsorbent along with adsorption temperature rising [41]. However, after temperature of 298K, the removal rate of GO/SA aerogel decreased as a result to the fact that increasing the temperature above that temperature leads to a weakening of the bond between the adsorbent and the adsorbate which induces the occurrence of the desorption process. The highest removal rates for GO/SA aerogel nanocomposites are (47.28%) at 75 minutes.

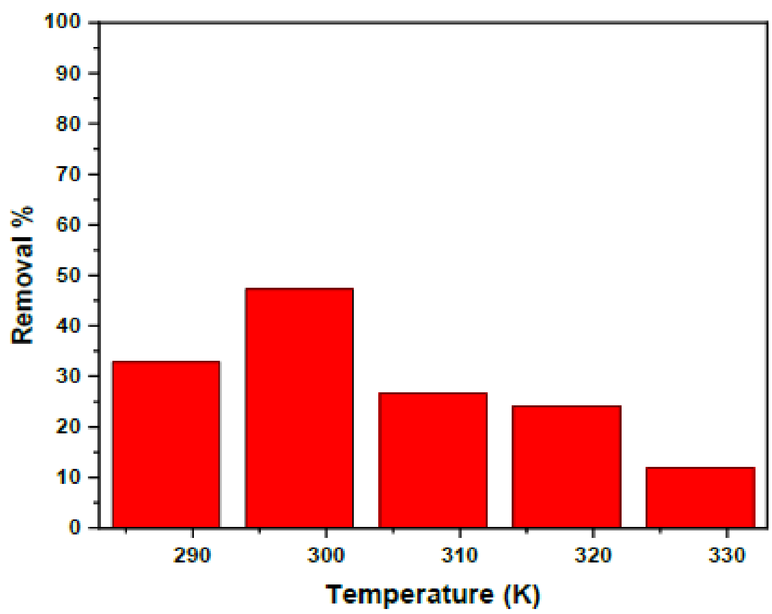

Figure 10: Effect of temperature on dye adsorption on the surface of GO/SA aerogel

Effect PH on Adsorption Process

The adsorption efficiency is influenced by the PH of solution. Therefore, one of the most important parameters investigated in this study was the acidity function. The adsorption efficiency of GO/SA aerogel was performed at different pH values 4,7 and 9 with the fixation of other parameters. The concentration of the dye solution was 20 ppm, the mass of the adsorbent (GO/SA) aerogel was 0.01 g, the temperature was 25 °C, and the adsorption time period was 75 min. The findings reveal that at pH 4 the removal percentage of methyl orange was 24%, however by raising the pH from 4 to 7, the adsorption efficiency has moderately decreased from 24% to 20% before increasing again to 33% at PH 9 as illustrated in Figure 11. The relatively variation of the removal rate values in the pH range was from 4 to 9, it can be attributed to the role of electrostatic interaction between adsorbent and adsorbate that affects the adsorption efficiency more than pH solution.

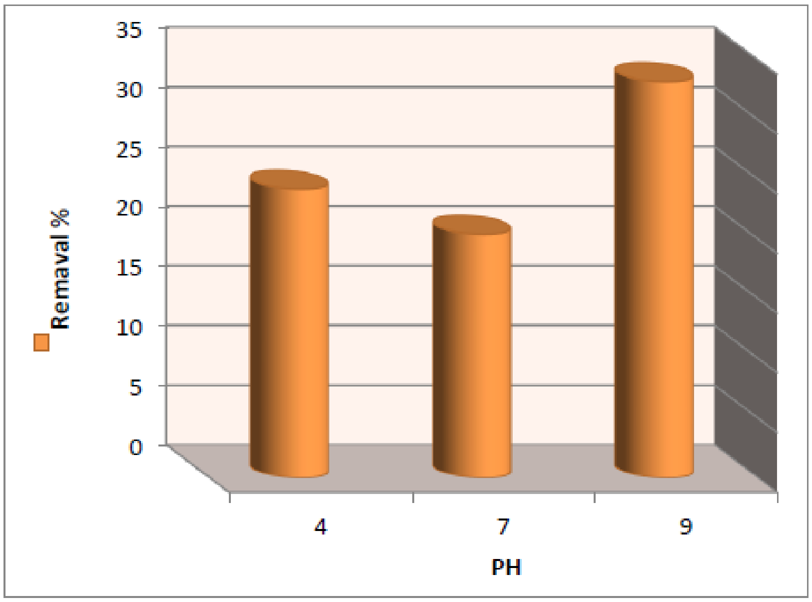

Figure 11: Effect of pH of the solution on dye adsorption on the surface of GO/SA aerogel.

Conclusions

Overall, GO/SA nanocomposite aerogel was prepared to be used as low cost efficient adsorbent to remove the methyl orange dye, one of the harmful polluting dyes from industrial wastewaters. Prepared GO/SA nanocomposite aerogel was characterized by analyzing FE-SEM, XRD and EDX, confirming the preparation of nanomaterial in addition to porous structure exhibition on surface. The adsorption performance of methyl orange dyes wastewater was investigated in this study. According to the results, time reaction, amount of adsorbent mass, initial methyl orange dye concentration, temperature and pH in solution have effects on the dye adsorption efficiency when prepared GO/SA nanocomposite aerogel is used. The highest removal percentage (92%). at the weight of (0.01 gm) for the GO/SA aerogel nanoparticles in short time (75 min) showed a good adsorption performance which qualified the of the GO/SA Aerogel nano composite to be economically low cost and efficient adsorbent for treating industrial wastewater dyes. With increasing initial adsorbate concentration from 2-20ppmL, the removal efficiency percentage was decreased from 89% to 25% suggesting saturation of active adsorptive site.

The other interesting result is that the adsorption of methyl orange dye onto two nano surfaces GO and GO/SA nanocomposite aerogel improved with increasing temperature revealing that the process is endothermic in nature. Meanwhile, the GO/SA nanocomposite aerogel exhibited a good removal percentage for methyl orange dyes. The current study has offered that the GO/SA nanocomposite aerogel can be used as a cheap adsorbent with high adsorption efficiency for dyes removal from industrial wastewaters which will achieve environmental benefits. In addition, it can be considered as an appropriate method to remove of the contamination of wastewater.

References

[1] Montazer-Rahmati, M.M., Rabbani, P., Abdolali, A. and Keshtkar, A.R., 2011. Kinetics and equilibrium studies on biosorption of cadmium, lead, and nickel ions from aqueous solutions by intact and chemically modified brown algae. Journal of hazardous materials, 185(1), pp.401-407.

[2] Yagub MT, Sen TK, Afroze S, et al. Dye and its removal from aqueous solution by adsorption: a review. Adv Colloid Interf Sci 2014; 209: 172–184.

[3] Ali, A.F.; Atwa, S.M.; El-Giar, E.M. Development of Magnetic Nanoparticles for Fluoride and Organic Matter Removal fromDrinking Water. In Water Purification; Elsevier: Amsterdam, The Netherlands, 2017; pp. 209–262.

[4] Krishna, P.G.; Chandra Mishra, P.; Naika, M.M.; Gadewar, M.; Ananthaswamy, P.P.; Rao, S.; Boselin Prabhu, S.R.; Yatish, K.V.;Nagendra, H.G.; Moustafa, M.; et al. Photocatalytic Activity Induced by Metal Nanoparticles Synthesized by Sustainable Approaches: A Comprehensive Review. Front. Chem. 2022, 10, 917831. [CrossRef]

[5] Luan, J.; Hou, P.-X.; Liu, C.; Shi, C.; Li, G.-X.; Cheng, H.-M. Efficient Adsorption of Organic Dyes on a Flexible Single-Wall Carbon Nanotube Film. J. Mater. Chem. A 2016, 4, 1191–1194. [CrossRef]

[6] Gouthaman, A.; Azarudeen, R.S.; Gnanaprakasam, A.; Sivakumar, V.M.; Thirumarimurugan, M. Polymeric Nanocomposites for the Removal of Acid Red 52 Dye from Aqueous Solutions: Synthesis, Characterization, Kinetic and Isotherm Studies. Ecotoxicol. Environ. Saf. 2018, 160, 42–51. [CrossRef]

[7] Naushad, M.; Ahamad, T.; AlOthman, Z.A.; Al-Muhtaseb, A.H. Green and Eco-Friendly Nanocomposite for the Removal of Toxic Hg(II) Metal Ion from Aqueous Environment: Adsorption Kinetics & Isotherm Modelling. J. Mol. Liq. 2019, 279, 1–8.

[8] Kooh, M.R.R.; Thotagamuge, R.; Chou Chau, Y.F.; Mahadi, A.H.; Lim, C.M. Machine Learning Approaches to Predict Adsorption Capacity of Azolla pinnata in the Removal of Methylene Blue. J. Taiwan Inst. Chem. Eng. 2022, 132, 104134. [CrossRef]

[9] Rathi BS and Kumar PS. Application of adsorption process for effective removal of emerging contaminants from water and wastewater. Environ Pollut 2021; 280: 116995.

[10] Monama GR, Mdluli SB, Mashao G, et al. Palladium deposition on copper(II) phthalocyanine/metal organic framework composite and electrocatalytic activity of the modified electrode towards the hydrogen evolution reaction. Renew Energ 2018; 119: 62–72.

[11] Sham AYW and Notley SM. Adsorption of organic dyes from aqueous solutions using surfactant exfoliated graphene. J Environ Chem Eng 2018; 6(1): 495–504.

[12] Guo, H., Jiao, T., Zhang, Q., Guo, W., Peng, Q., Yan, X., 2015. Preparation of graphene oxide-based hydrogels as efficient dye adsorbents for wastewater treatment. Nanoscale Research Letters 10, 1-10.

[13] Geim AK. Graphene: status and prospects. Science. 2009;324:1530–4.

[14] Huang X, Qi X, Boey F, Zhang H. Graphene-based composites. Chem Soc Rev. 2012;41:666–86.

[15] Geim AK, Novoselov KS. The rise of graphene. Nature Mater. 2007;6:183–91.

[16] Hummers Jr,W.S.; Offeman, R.E. Preparation of graphitic oxide. J. Am. Chem. Soc. 1958, 80, 1339.

[17] Petosa, A.R., Jaisi, D.P., Quevedo, I.R., Elimelech, M., Tufenkji, N., 2010. Aggregation and deposition of engineered nanomaterials in aquatic environments: Role of physicochemical interactions. Environ. Sci. Technol. http://dx.doi.org/10.1021/es100598h.

[18] Yang, H., Cui, H., Tang, W., Li, Z., Han, N., Xing, F., 2017a. A critical review on research progress of graphene/cement based composites. Composites A 102, 273–296. http://dx.doi.org/10.1016/j.compositesa.2017.07.019.

[19] Korkmaz, S.; Kariper, ˙I.A. Graphene and graphene oxide based aerogels: Synthesis, characteristics and supercapacitor applications. J. Energy Storage 2020, 27, 101038. [CrossRef]

[20] Xing, R., Wang, W., Jiao, T., Ma, K., Zhang, Q., Hong, W., Qiu, H., Zhou, J., Zhang, L., Peng, Q., 2017. Bioinspired Polydopamine Sheathed Nanofibers Containing Carboxylate Graphene Oxide Nanosheet for High-Efficient Dyes Scavenger. ACS Sustainable Chemistry & Engineering 5, 4948–4956.

[21] H., Jiao, T., Zhang, L., Zhou, J., Zhang, Q., Peng, Q., Yan, X., 2015. Preparation and adsorption capacity evaluation of graphene oxide-chitosan composite hydrogels. Science China Materials 58, 811–818.

[22] Zhao, Y.; Hu, C.G.; Song, L.; Wang, L.X.; Shi, G.Q.; Dai, L.M.; Qu, L.T. Functional graphene nanomesh foam. *Energy Environ. Sci.* 2014, *7*, 1913–1918

[23] Gao, C.; Wang, X.-L.; An, Q.-D.; Xiao, Z.-Y.; Zhai, S.-R. Synergistic preparation of modified alginate aerogel with melamine/chitosan for efficiently selective adsorption of lead ions. Carbohydr. Polym. 2021, 256, 117564. [CrossRef]

[24] Lee, I.; Kang, S.-M.; Jang, S.-C.; Lee, G.-W.; Shim, H.E.; Rethinasabapathy, M.; Roh, C.; Huh, Y.S. One-pot gamma ray-induced green synthesis of a Prussian blue-laden polyvinylpyrrolidone/reduced graphene oxide aerogel for the removal of hazardous pollutants. J. Mater. Chem. A 2019, 7, 1737–1748. [CrossRef]

[25] Lyu,W.; Li, J.; Zheng, L.; Liu, H.; Chen, J.; Zhang,W.; Liao, Y. Fabrication of 3D compressible polyaniline /cellulose nanofiber aerogel for highly efficient removal of organic pollutants and its environmental-friendly regeneration by peroxydisulfate process.Chem. Eng. J. 2021, 414, 128931.

[26] Esmaeili, Z.; Izadyar, S.; Hamzeh, Y.; Abdulkhani, A. Preparation and Characterization of Highly Porous Cellulose Nanofibrils/ Chitosan Aerogel for Acid Blue 93 Adsorption: Kinetics, Isotherms, and Thermodynamics Analysis. J. Chem. Eng. Data 2021,66, 1068–1080.

[27] Nita, L.E.; Ghilan, A.; Rusu, A.G.; Neamtu, I.; Chiriac, A.P. New trends in bio-based aerogels. Pharmaceutics 2020, 12, 449.

[28] Maleki, H. Recent advances in aerogels for environmental remediation applications: A review. Chem. Eng. J. 2016, 300, 98–118.

[29] Hecht D.S., Hu L., Irvin G. Emerging transparent electrodes based on thin films of carbon nanotubes, graphene, and metallic nanostructures. Adv. Mater. 2011;23:1482–1513.

[30] Manna, S., Bhattacharya, S., Sengupta, S., Das, P., 2018. Synthesis of graphene oxide dots coated biomatrices and its application for the removal of multiple pollutants present in wastewater. J. Clean. Prod. http://dx.doi.org/10.1016/j.jclepro.2018.08.261.

[31] Zhuo, H. et al. A supercompressible, elastic, and bendable carbon aerogel with ultrasensitive detection limits for compression strain, pressure, and bending angle. Adv. Mater. 30, 1706705 (2018).

[32] Liu, J. et al. Superelastic and multifunctional graphene-based aerogels by interfacial reinforcement with graphitized carbon at high temperatures. Carbon 132, 95–103 (2018).

[33] Sun, H., Xu, Z. & Gao, C. Multifunctional, ultra-flyweight, synergistically assembled carbon aerogels. Adv. Mater. 25, 2554–2560 (2013).

[34] X.-Y. Dai, L.-M. Kong, X.-L. Wang, Q. Zhu, K. Chen, and T. Zhou, "Preparation, characterization and catalytic behavior of pectinase covalently immobilized onto sodium alginate/graphene oxide composite beads," Food Chemistry, vol. 253, pp. 185-193, 2018/07/01/ 2018.

[35] - C. Jiao et al., "Sodium alginate/graphene oxide aerogel with enhanced strength-toughness and its heavy metal adsorption study," Int J Biol Macromol, vol. 83, pp. 133-41, Feb 2016.

[36] - L. Sun and B. Fugetsu, "Graphene oxide captured for green use: Influence on the structures of calcium alginate and macroporous alginic beads and their application to aqueous removal of acridine orange," Chemical Engineering Journal, vol. 240, pp. 565-573, 2014/03/15/ 2014.

[37] Dutta, M. J. & Manna, I. Laser processing of materials. Sadhana 28, 495–562 (2003).

[38] A. R. Laftah, "New Synthesis of BaO nanoparticles Using the UV-Irradiation Technique for removal cibacron blue dye from their aqueous solution," Egyptian Journal of Chemistry, vol. 65, no. 13, 2022.

[39] Y. Liu, "Adsorption and release kinetics, equilibrium, and thermodynamic studies of hymexazol onto diatomite," ACS omega, vol. 5, no. 45, pp. 29504-29512, 2020.

[40] M. S. M. Zaini, "Adsorption Isotherm and Kinetic Study of Methane on Palm Kernel Shell-Derived Activated Carbon," Journal of Bioresources and Bioproducts, vol. 8, no. 1, pp. 66-77, 2023.

[41] H. A. Alshamsi, "Adsorption isotherms, kinetic modeling and thermodynamics of toxic crystal violet from aqueous solution on eco-friendly L-cysteine-reduced graphene oxide," AIP Conference Proceedings, vol. 2394, no. 1, p. 40034, 2022.